

NASA/TM—2004—212067



Automated Static Culture System Cell Module Mixing Protocol and Computational Fluid Dynamics Analysis

*Stanley J. Kleis, Ph.D.
University of Houston*

*Tuan Truong
Lyndon B. Johnson Space Center*

*Thomas J. Goodwin, Ph.D.
Lyndon B. Johnson Space Center*

January 2004

THE NASA STI PROGRAM OFFICE ... IN PROFILE

Since its founding, NASA has been dedicated to the advancement of aeronautics and space science. The NASA Scientific and Technical Information (STI) Program Office plays a key part in helping NASA maintain this important role.

The NASA STI Program Office is operated by Langley Research Center, the lead center for NASA's scientific and technical information. The NASA STI Program Office provides access to the NASA STI Database, the largest collection of aeronautical and space science in the world. The Program Office is also NASA's institutional mechanism for disseminating the results of its research and development activities. These results are published by NASA in the NASA STI Report Series, which includes the following report types:

- **TECHNICAL PUBLICATION.** Reports containing completed research or major significant phases of research. Also presents the results of NASA programs (including extensive data or theoretical analysis). Includes compilations of significant scientific and technical data and information deemed to be of continuing reference value. This is the NASA equivalent of peer-reviewed, formal, professional papers, but has less stringent limitations on manuscript length and extent of graphic presentations.
- **TECHNICAL MEMORANDUM.** Scientific and technical findings that are preliminary or of specialized interest. For example, quick release reports, working papers, and bibliographies that contain minimal annotation. Does not contain extensive analysis.
- **CONTRACTOR REPORT.** Scientific and technical findings by NASA-sponsored contractors and grantees.

- **CONFERENCE PUBLICATION.** Collected papers from scientific and technical conferences, symposia, seminars, or other meetings sponsored or cosponsored by NASA.
- **SPECIAL PUBLICATION.** Scientific, technical, or historical information from NASA programs, projects, and missions, often concerned with subjects having substantial public interest.
- **TECHNICAL TRANSLATION.** English-language translations of foreign scientific and technical material pertinent to NASA's mission.

Specialized services that complement the STI Program Office's diverse offerings include creating custom thesauri, building customized databases, organizing and publishing research results, and even providing videos.

For more information about the NASA STI Program Office, see the following:

Access the NASA STI Program Home Page at <http://www.sti.nasa.gov>.

E-mail your question via the Internet to help@sti.nasa.gov.

Fax your question to the NASA STI Help Desk at (301) 621-0134.

Telephone the NASA STI Help Desk at (301) 621-0390.

Write to:

NASA Access Help Desk
NASA Center for AeroSpace Information
7121 Standard Drive
Hanover, MD 21076-1320

NASA/TM—2004—212067



Automated Static Culture System Cell Module Mixing Protocol and Computational Fluid Dynamics Analysis

*Stanley J. Kleis, Ph.D.
University of Houston*

*Tuan Truong
Lyndon B. Johnson Space Center*

*Thomas J. Goodwin, Ph.D.
Lyndon B. Johnson Space Center*

National Aeronautics and
Space Administration

Johnson Space Center
Houston, Texas 77058-3696

January 2004

Available from:

NASA Center for Aerospace Information
7121 Standard Drive
Hanover, MD 21076-1320

National Technical Information Service
5285 Port Royal Road
Springfield, VA 22161

This report is also available in electronic form at <http://ston.jsc.nasa.gov/collections/NTRS>

Contents

	Page
Abstract	1
Introduction	1
Proposed Protocol.....	2
Analysis	3
Mathematical Model	6
Simplified Problem.....	7
Numerical Methods.....	9
Results	9
Concentration Distributions	9
Bag Mixing Process.....	11
Effect of H on Mixing.....	12
Effects of Amplitude of Oscillation on Mixing	19
Shear Levels	21
Velocity	23
References	24

Table

1	Maximum Wall Shear Stress Levels and Computed Velocity Parameters.....	21
---	--	----

Figures

1	Top and side views of proposed ASCS bag assembly	2
2	Bag with partition	3
3	Scalar concentration flux in a strain rate field	5
4	Velocity above an oscillating plate.....	6
5	Simplified geometry	8

Contents

(continued)

	Page
6 Oxygen patch diffusion with no flow in first 2 hrs	10
7 Relative oxygen concentration contours on center plane	13
8 Relative oxygen concentration contours on bag wall.....	14
9 Relative oxygen concentration contours on center plane	15
10 Relative oxygen concentration contours on bag wall.....	16
11 Relative oxygen concentration contours on center plane	17
12 Relative oxygen concentration contours on bag wall.....	18
13 Relative oxygen concentration contours.....	19
14 Relative oxygen concentration contours.....	20
15 Wall shear stress contours at maximum shear	22
16 Maximum wall shear stress versus flow velocity parameter.....	23

Abstract

This report is a documentation of a fluid dynamic analysis of the proposed Automated Static Culture System (ASCS) cell module mixing protocol. The report consists of a review of some basic fluid dynamics principles appropriate for the mixing of a patch of high oxygen content media into the surrounding media which is initially depleted of oxygen, followed by a computational fluid dynamics (CFD) study of this process for the proposed protocol over a range of the governing parameters. The time histories of oxygen concentration distributions and mechanical shear levels generated are used to characterize the mixing process for different parameter values.

Introduction

The ASCS is being developed for use on the International Space Station to support cell science experiments in a microgravity environment. As shown in Figure 1, the proposed culture bag design consists of a rigid header block with two access ports for cell culture inoculation and sampling and a flexible bag material, sealed to the header. Each header block will also have a fluid transfer line for automated media exchange. The ASCS will have multiple modules with each module consisting of three or more bag assemblies. The proposed bag dimensions are 6.45 cm (2.54") from header to bag tip, 4.65 cm (1.83") wide at the header, and 0.76 cm (0.30") high at the header. This gives a nominal volume of 10 ml of media inside each bag.

A mixing protocol is needed for these static culture bags to distribute inoculum, infused fresh media, or other media treatments as uniformly as possible throughout the bag medium volume. In the absence of external mixing, a highly nonuniform distribution of environmental parameters and cell number density will result, leading to poor cell growth and compromised cell science experimental results. Thus, the mixing protocol should be used each time media exchange or other treatments are made. It may also be desirable to provide periodic mixing of the bag contents during normal culture times to redistribute cells and/or environmental variables within the bag.

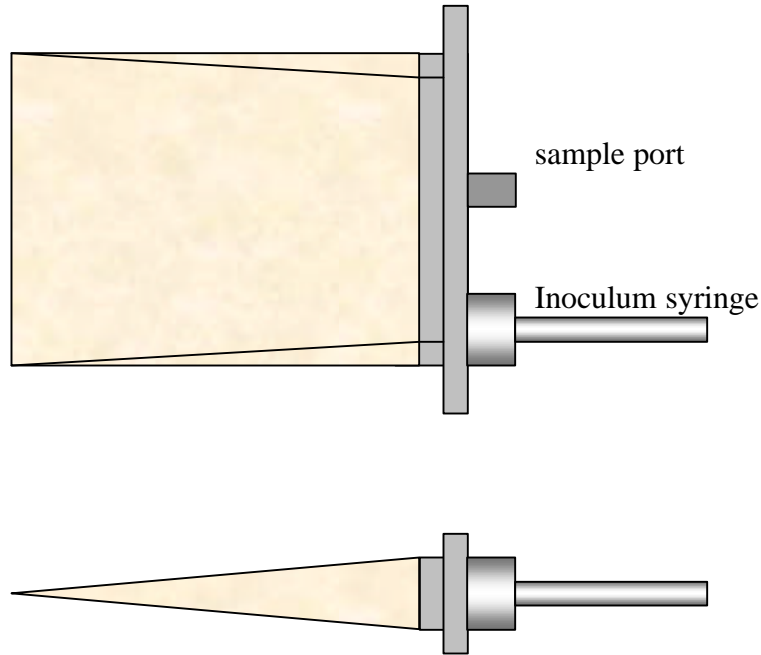


Figure 1. Top and side views of proposed ASCS bag assembly.

The mixing protocol must provide a good distribution of the infused scalar throughout the bag volume, but must also produce low mechanical stress levels, to avoid damaging the shear sensitive mammalian or other types of cells. Since the system is designed for nominally static cultures, the mixing is expected to be done only for short periods following infusion.

Proposed Protocol

The proposed protocol consists of partially dividing the bag to form a U-shaped structure either by 1) a fixed partition or 2) applying pressure along the bag centerline to completely seal one leg of the bag from the other as shown in Figure 2. Then, by applying pressure alternately to the bag surface on either side of the partition, a back-and-forth flow can be induced from one side of the bag to the other around the end of the partition.

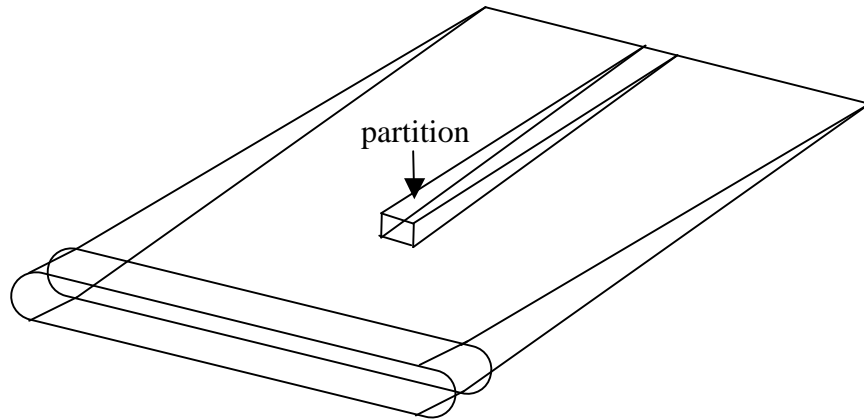


Figure 2. Bag with partition.

Note: The present analysis will assume there is sufficient volume of media in the bag that the prescribed displaced volume is available as each side of the bag is squeezed. This requirement may have to be met by carefully maintaining the proper volume of media in the bag by adding or removing media through the fluid transfer tube after inoculation or sampling and during the periodic feeding. It will also be assumed that the mechanism for applying the pressure to the bag surfaces will have motion limits to prevent crushing of cellular material in the bag legs.

Analysis

The oscillatory motion of fluid in the main region between the partition tip and the header can cause two types of mixing. If the flow is vigorous enough it could become turbulent, resulting in very efficient mixing, but with possibly high shear stresses. At lower rates of oscillation, the flow would be laminar, but unsteady. To determine the nature of the flow, the flow Reynolds number must be estimated. The flow Reynolds number, Re , is given by $Re = UL/v$, where U and L are characteristic velocity and length scales and v is the media kinematic viscosity. Since the proposed bag geometry is long and wide compared with the height, the proper length scale for the flow is the bag height.

The value for this design is the maximum height of $L = 0.76$ cm. The characteristic velocity can be found from the peak volume flow rate of the displaced fluid divided by the flow cross-sectional area. Choosing to displace one-fourth of the bag volume in 1 second, the Reynolds number can be estimated as

$$\text{Re} = \frac{UL}{\nu} = \frac{QL}{An} = \frac{QL}{Lw/2n} = \frac{2.5\text{cm}^3}{s} \frac{1}{2.34\text{cm}} \frac{1}{1.12 \times 10^{-2} \text{cm}^2 / \text{s}} = 96$$

where the area has been estimated as the bag height times half the bag width (one leg width). This value of Reynolds number is far below the laminar-turbulent transition value for a channel flow (several thousand) [1]. Thus, the flow could be expected to be laminar; however, the flow might separate around the partition end, possibly resulting in a shear layer, which could be unstable and/or turbulent. To properly handle this possibility, a simple turbulence model was used for all CFD calculations.

For the laminar flow situation, mixing of a scalar is a diffusion process augmented by convective transport. Since the diffusivity will be nearly constant for the conditions of the bag, the diffusive flux will be proportional to the local scalar concentration gradient. To enhance the mixing process, the local scalar concentration gradient can be made steeper by inducing a velocity gradient in the direction of the scalar flux. To understand this process, consider a uniform patch of high-concentration fluid next to a solid boundary as shown in Figure 3. The fluid will stick to the wall, forming a velocity boundary layer with zero velocity at the wall and velocity increasing with distance from the wall. The scalar will tend to move with the fluid, resulting in the straining of the initial patch into the flow direction. This straining motion creates a steeper concentration gradient normal to the surface, with enhanced diffusive transport of the scalar away from the surface at the initial location and transport toward the surface under the patch downstream. As the original fluid patch is elongated, the patch width must decrease to maintain constant volume. This narrowing steepens the concentration gradient normal to the surface, increasing the diffusive flux out of the patch, into the adjacent fluid. At the same time, the surface area over which diffusion takes place is constantly increasing due

to the straining motion. Both of these effects result in greatly enhanced mixing of the patch into the surroundings.

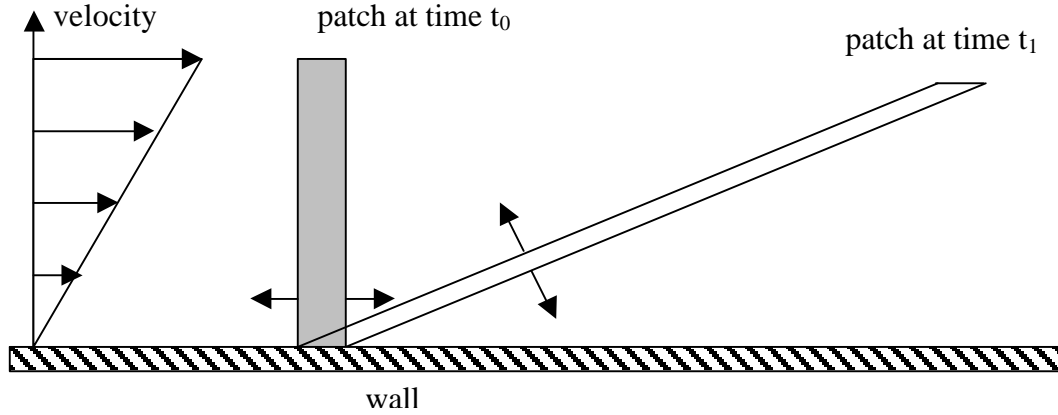


Figure 3. Scalar concentration flux in a strain rate field.

In a nearly two-dimensional flow like the bag, the enhancement of the diffusive transport is primarily in a direction normal to the wall. This means that best results can be expected when convective transport is used to move fluid across the bag (in the long dimensions) and allow enough time for diffusive transport toward and away from the walls (in the short-dimension direction).

The effects of the strain rate field will be most effective when the velocity gradient extends across the entire height of the gap. This distance can be estimated for the oscillatory flow in the bag by considering the classic unsteady Stokes flow above an oscillating flat plate, where a plate is oscillated along its length in a steady harmonic motion (Stoke's second problem [1]) (see Figure 4).

The solution for the velocity field as a function of distance above the plate is

$$u(y) = Ue^{-y\sqrt{\frac{\omega}{2\nu}}} \sin(\omega t - y\sqrt{\frac{\omega}{2\nu}}).$$

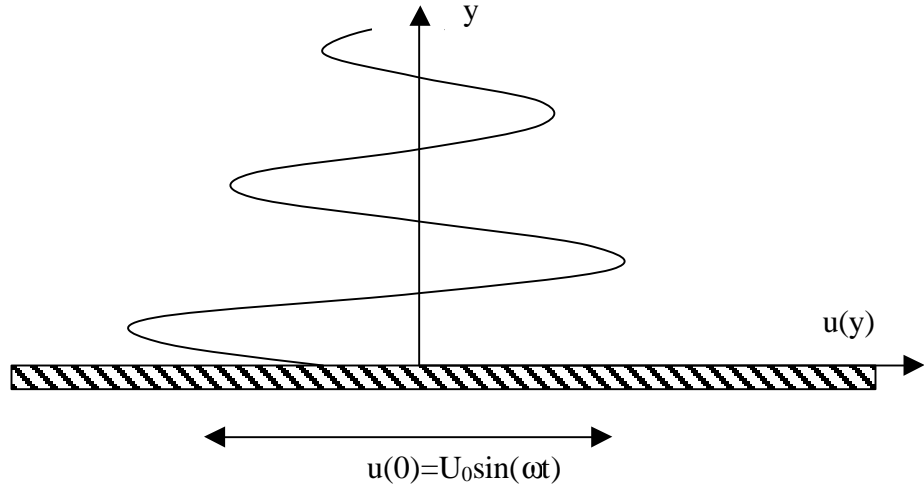


Figure 4. Velocity above an oscillating plate.

Thus, the length scale normal to the wall is the viscous wavelength, $\lambda = 2\pi\sqrt{\frac{2\nu}{\omega}}$, where ω is the angular frequency in radians/s. For the ASCS bag at a frequency of 1 Hz, the length scale is 3.75 mm, which is comparable to the distance from the wall to the centerline of the bag. This means that, for frequencies much higher than 1 Hz, the flow will have steep velocity gradients near the wall and a more nearly uniform flow away from the wall, while flows at lower frequencies will have significant velocity gradients across the entire domain. That is, it will be best for mixing to operate in the range of 1 Hz or lower frequencies.

The flow in the ASCS bag using the proposed protocol is obviously more complex than these simple examples. However, these limiting cases do provide reasonable initial estimates for the operating parameters and a basic understanding of the physical mechanisms involved in the mixing process. The full problem will be solved for a range of parameters using CFD for a more realistic, yet still somewhat simplified geometry.

Mathematical Model

Since the geometry of the bag was specified, there are only three main parameters to be varied in this study: the partition location, the frequency of oscillation, and the

amplitude of the oscillation. The partition location will be specified by the distance from the partition tip to the header block, H . The frequency of oscillation, f , will be specified in Hz. The amplitude of oscillation, V , will be specified in terms of one half of the volume of fluid displaced from each leg from full expansion to full compression.

The flow field must satisfy the continuity and Navier Stokes equations subject to appropriate boundary conditions. The only parameter from the governing equations is the Reynolds number described previously. The scalar concentration field must further satisfy the scalar transport equation. This solution depends upon the Schmidt number, $Sc = \nu/D$, and Reynolds number, where D is the binary scalar diffusivity. For the current study, a value of $D = 2.5 \times 10^{-6} \text{ m}^2/\text{s}$ [2] is used to characterize the diffusion of oxygen into water (assumed the same as culture medium). This gives a value of $Sc = 452$ for all cases.

The full solution of the problem would require detailed knowledge of the bag boundary motion at all times. For the deformable bag, this information is not known. One possible approach would be to arbitrarily specify a bag surface motion and then solve the problem for a deformable region as a function of time. This approach is complex, time-consuming, and deemed unnecessary for design purposes. Instead, a much simpler problem was solved as an approximation to the full bag problem.

Simplified Problem

The main volume of the bag and the region that is expected to be the hardest to mix is the region near the header block. This region has the largest gap and lowest velocities (smallest relative displacements). For the fluid motion in the main bag region, the bag legs act as fluid sources and sinks and are the regions of bag boundary deformation. Thus, parts of the bag legs are replaced in the simplified model by constant height sections with flow inlets at the far ends. The computational domain for the simplified model is shown in Figure 5. The inlets, on the right-hand ends of the two legs in Figure 5, have periodic uniform velocities imposed out of phase with each other to maintain constant fluid volume in the bag at all times.

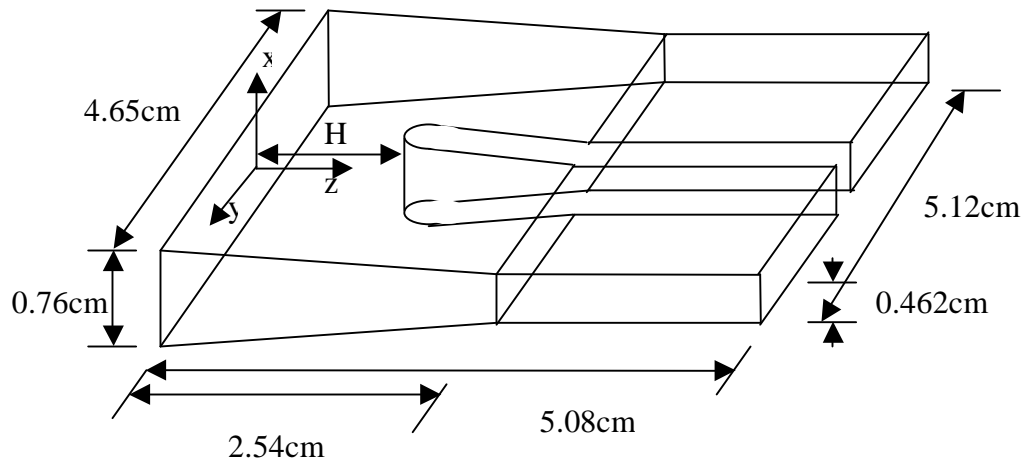


Figure 5. Simplified geometry (partition gap 0.508 cm wide).

Note: Flat wall surfaces, except the partition tip, are used to reduce numerical computation time. The partition tip has a 0.254-cm radius.

The purpose of the constant height extensions on each leg of the bag is to provide regions to collect the outflow from the main bag section, which would then be reinjected into the main section during the next half cycle of the flow oscillation. This is in some ways similar to the actual deformable bag, although the mixing within this region is expected to be less than in the actual bag. The height of the leg extensions was chosen to approximate the time-averaged height of the actual bag leg.

Note: Details of the mixing will be different between the model and actual bag in the extension regions. Exercise care when interpreting results in this region, although the actual bag is likely to provide better mixing than the model in these regions.

Boundary conditions for the velocity field are no-slip, no-penetration conditions on all solid surfaces and the uniform periodic flows at the leg extension ends just described, the flow field assumed to start from rest. The scalar concentration field is subject to zero

diffusive flux on all surfaces and assumed to start with zero concentration of oxygen everywhere except in a small patch of fluid started at saturated conditions as described below.

Numerical Methods

The commercial software package FLUENT was used to solve for the velocity and scalar concentration distributions in the bag as functions of time. The full Reynolds averaged Navier Stokes and the scalar transport equations were solved with a standard k- ϵ turbulence model for the velocity and concentration fields. The open ends of the extended legs had "velocity inlet" boundary conditions [3] with user-defined functions [4] written in C language to implement the oscillatory uniform velocity conditions with zero scalar concentration gradient normal to the surfaces (zero scalar diffusion).

Results

In order to study the mixing characteristics, we dispersed a cylindrical-shaped patch of fluid that was initially saturated with oxygen, using the "patch" function, into the domain that was set to zero initial oxygen concentration. For all cases, the initial patch was cylindrical in shape oriented with its axis across the gap and 10 mm in diameter. The patch axis was generally started at 10 mm from the mid-plane (half-width location) and 5 mm from the header block ($y = 10$ mm, $z = 5$ mm).

Concentration Distributions

To aid in interpreting the results, the concentration was normalized by the saturation value throughout the study. All concentration values then represent the oxygen level relative to that at saturation.

Since the mixing process will be a function of position across the gap, relative concentration distributions were recorded as functions of time at two locations, at the wall and on a plane at the half-gap location ($x = 0$). Wall shear stress contours were also recorded to show the maximum shear levels in the fluid media.

The first case is that of pure diffusion to provide a reference for comparison of other results. The inlet velocities were zero. Still frames from the video are shown in Figure 6 for a few selected times. Even after nearly 2 hrs, the patch is still poorly mixed into the

surrounding media. The peak concentration is over 0.44 of saturation and a large portion of the media volume remains below 0.01 of saturation. This case clearly demonstrates the need for a mixing protocol for the ASCS bags.

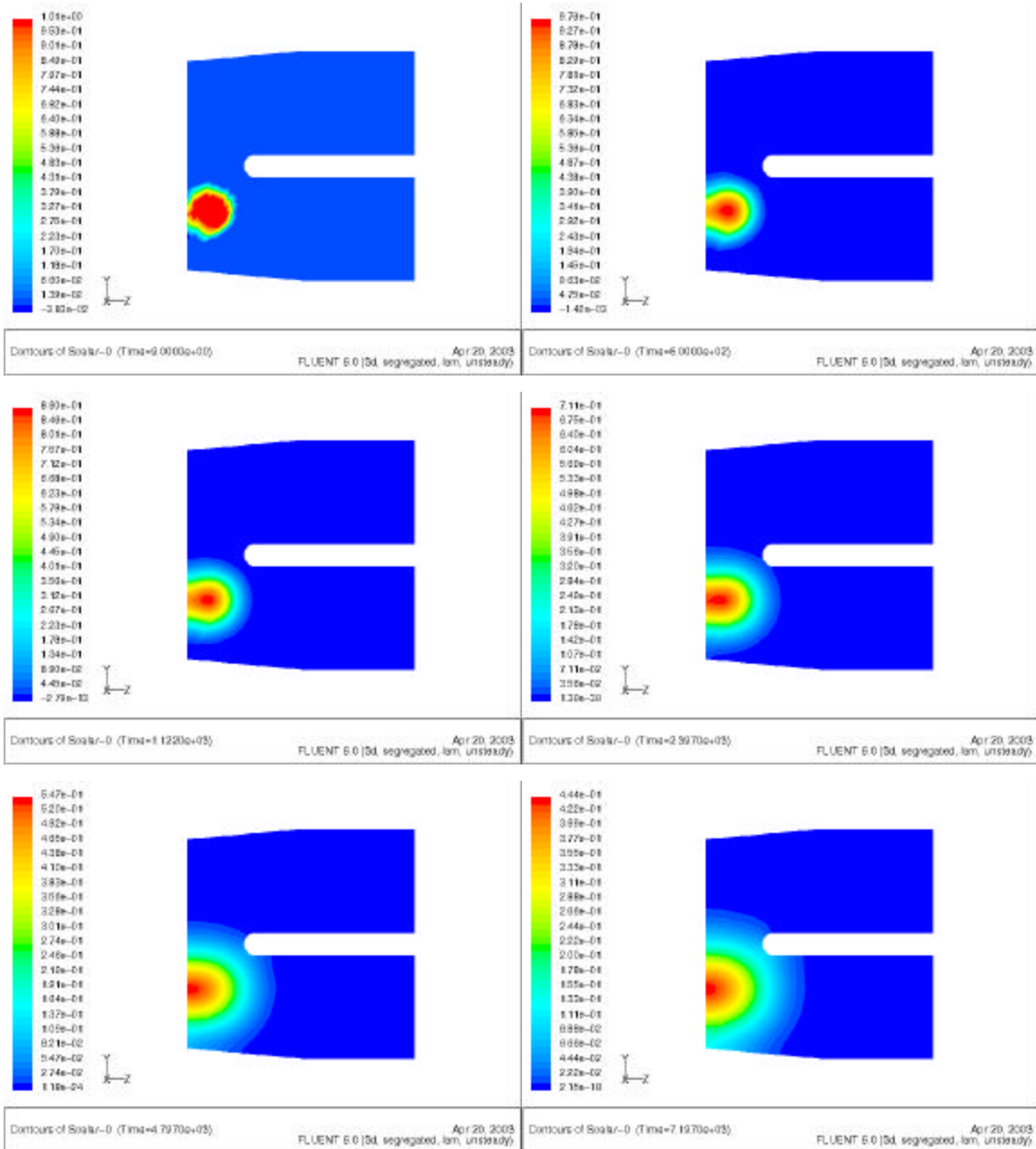


Figure 6. Oxygen patch diffusion with no flow in first 2 hrs.
Partition tip position $H = 1.27$ cm from header block.

The effects of partition gap, H , and the oscillation amplitude and frequency are interrelated because they all affect the overall patch displacement and fluid strain rates. Mixing should be enhanced by larger displacements and higher velocities, resulting in higher strain rates and larger diffusion surface area. However, increasing the frequency of oscillation holding the displaced volume constant will decrease the time for diffusion during one oscillation cycle. Therefore, each parameter needs to be investigated with respect to overall mixing efficiency.

Bag Mixing Process

Before exploring the effects of each parameter, the overall flow pattern and mixing process in the model system should be understood. Shown in Figure 7 is the concentration distribution at one-half period time increments for the case of $H = 1.27$ cm, $f = 0.3$ Hz, and $V = 1.5$ cc. Time is increasing from left to right, then top to bottom. Thus, the left side figures are at even multiples of the oscillation period, while the right side figures are at odd half periods. Figure 8 shows the corresponding distributions at the bag surface.

Note: *The color-scale range changes between figures, to span the complete range of values at that time. Exercise care when comparing one distribution to another at a different time.*

The figures indicate a greatly improved mixing compared with the pure diffusion case shown above. In just 10 s, the maximum-to-minimum concentration range has dropped to about 14% of the initial range and the concentration uniformity has greatly improved, compared with 44% of saturation range at 2 hrs with no mixing protocol.

Comparing the contours at the half-gap location, Figure 7, with those at the bag wall, Figure 8, two additional mixing effects can be seen. As the flow progresses around the partition tip, a large-scale rotational motion is observed. This motion further increases the surface area for diffusion and transports fluid across the bag. Second, the high-concentration regions in the half-gap plane move outward, away from the partition tip toward the header block. The bag surface contours indicate a transport in the opposite direction, from the outer surfaces toward the partition. Thus, there is a secondary flow of

fluid toward the half-gap plane at the partition coming from the bag surfaces. This is driven by the pressure gradient associated with the curvature of flow around the partition tip. The higher-speed flow on the half-gap plane is thrown outward by centrifugal force creating a pressure gradient across the flow, while the low-momentum fluid near the bag surfaces is driven toward the center of curvature by this pressure gradient. This effect can be seen in Figure 7 as higher-concentration fluid appears near the partition in the last three figures. This vertical transport of fluid greatly enhances the overall mixing efficiency.

Note: *Contours that reach the flow inlets at the bag leg ends are distorted on the return cycle due to the zero gradient (zero diffusion) conditions imposed on these boundaries. Care must be exercised when interpreting the returned flow from these regions. Only the fluid that has not left the computational domain should be considered for interpretation. These areas can be identified by nearly horizontal contours extending from the inlets into the bag leg.*

Effects of H on Mixing

Smaller H will increase the averaged fluid velocity through the partition gap. An increased velocity will have the direct effect of increased strain rates and also can change the flow pattern. Figures 9 and 10 show the concentration contours for the conditions $H = 0.76$ cm, $f = 0.3$ Hz, and $V = 1.5$ cc. The most noticeable difference, when compared with the previous case, is in the strength of the circulatory motion induced by the higher velocity through the narrower gap at the partition tip. This increased rotation enhances the overall mixing process, resulting in a range of concentrations at 9.99 s of 0.11 versus 0.14 for $H = 1.27$ cm. This is a relatively small improvement for a 40% decrease in gap width. The effect of gap width on shear levels is shown below.

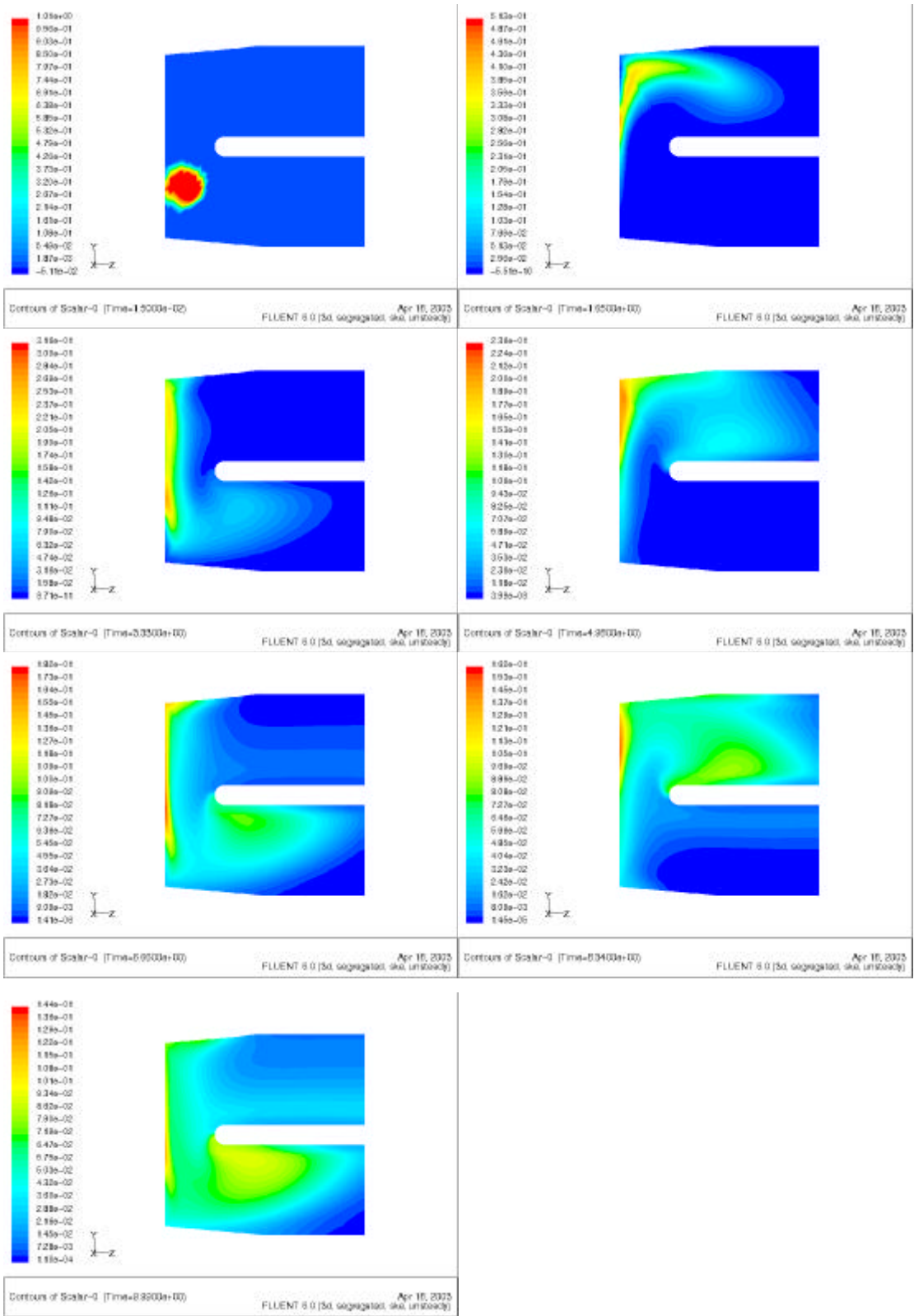


Figure 7. Relative oxygen concentration contours on center plane.

$H = 1.27 \text{ cm}$, $f = 0.3 \text{ Hz}$, $V = 1.5 \text{ cc}$.

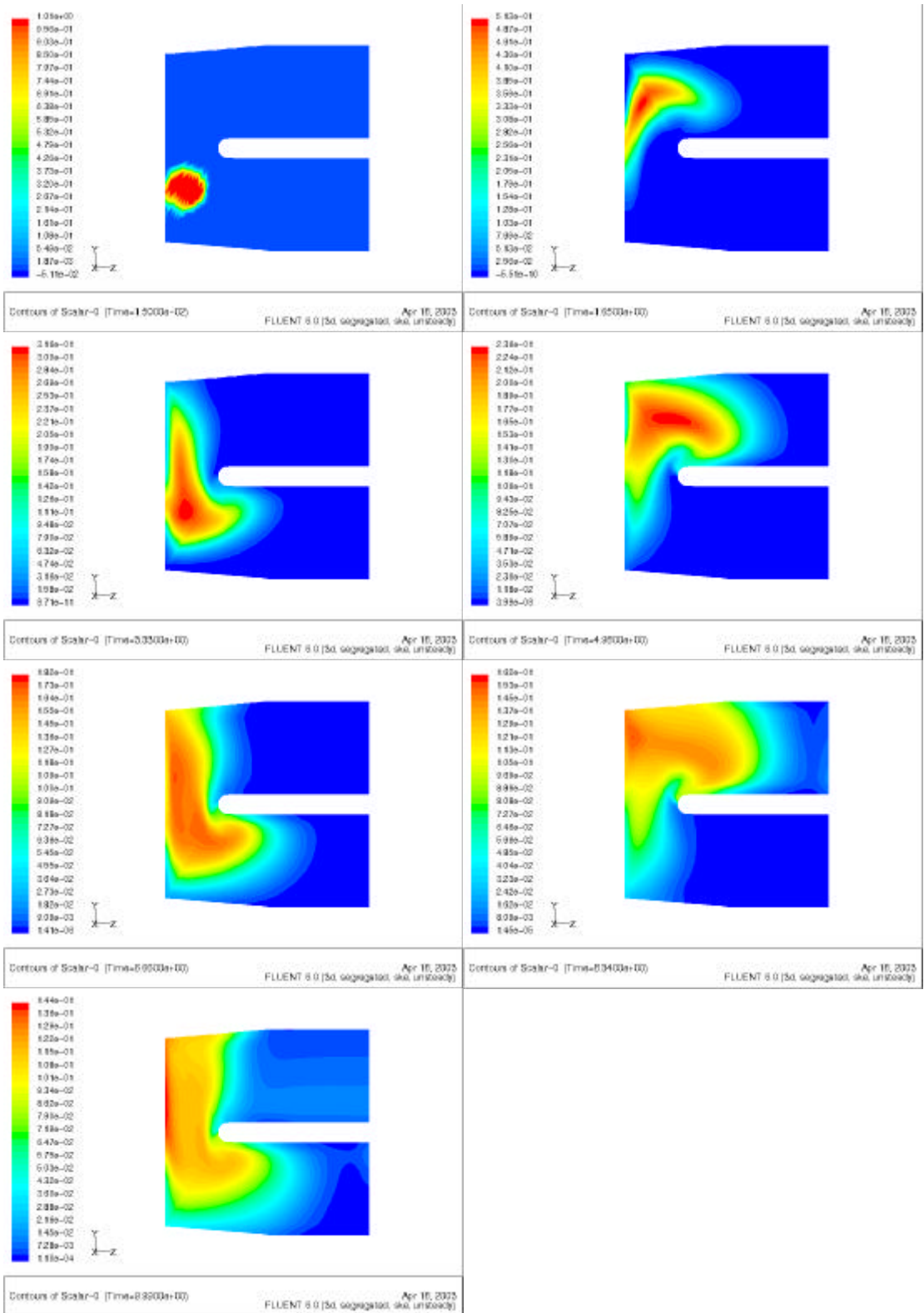


Figure 8. Relative oxygen concentration contours on bag wall.

$H = 1.27$ cm, $f = 0.3$ Hz, $V = 1.5$ cc.

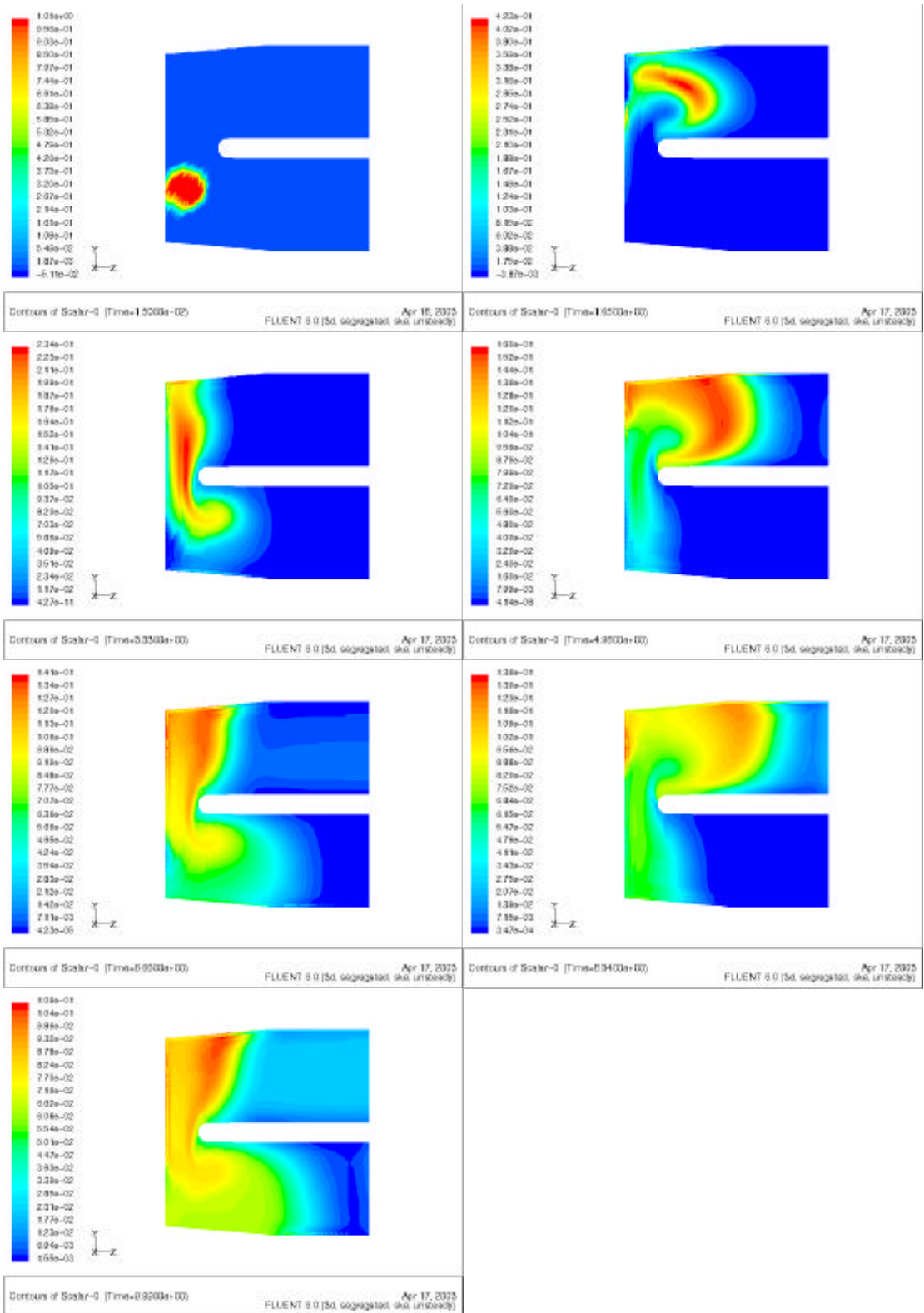


Figure 9. Relative oxygen concentration contours on center plane.

$H = 0.76$ cm, $f = 0.3$ Hz, $V = 1.5$ cc.

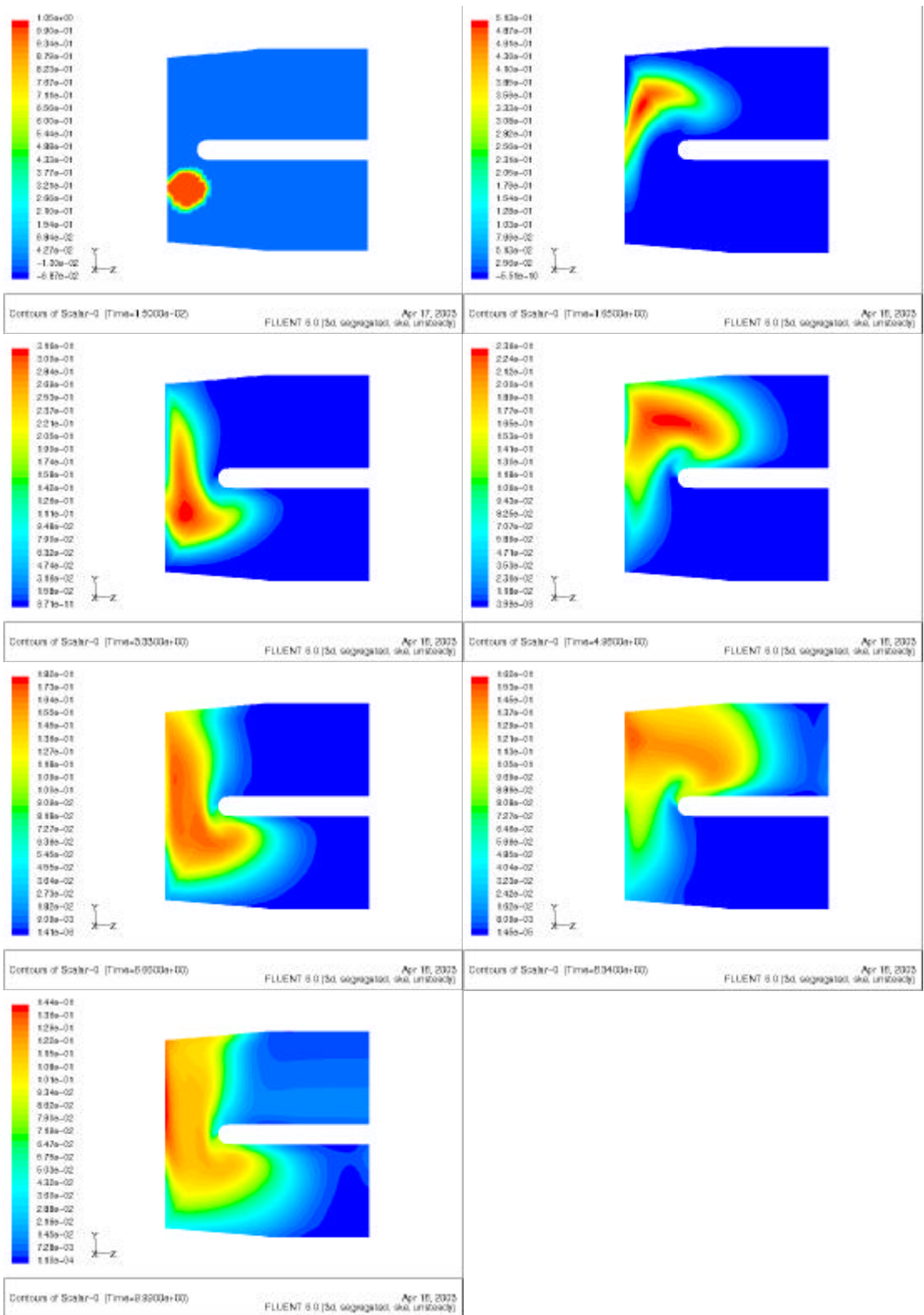


Figure 10. Relative oxygen concentration contours on bag wall.

$H = 0.76 \text{ cm}$, $f = 0.3 \text{ Hz}$, $V = 1.5 \text{ cc}$.

Effects of Frequency on Mixing

As previously discussed, the mixing process depends upon the strain rates imposed by the oscillatory flow. The strain rates will scale with the frequency of oscillation for a given maximum volume of flow displacement. Figures 11 and 12 show the concentration contours at $\frac{1}{2}$ -s intervals for $H = 1.27$ cm, $f = 1.0$ Hz, and $V = 1.5$ cc for the center plane and bag walls, respectively. At the end of only 5 s, the range of concentrations has reduced to 12% of saturation, compared with the 14% at 10 s for the $f = 0.3$ Hz case.

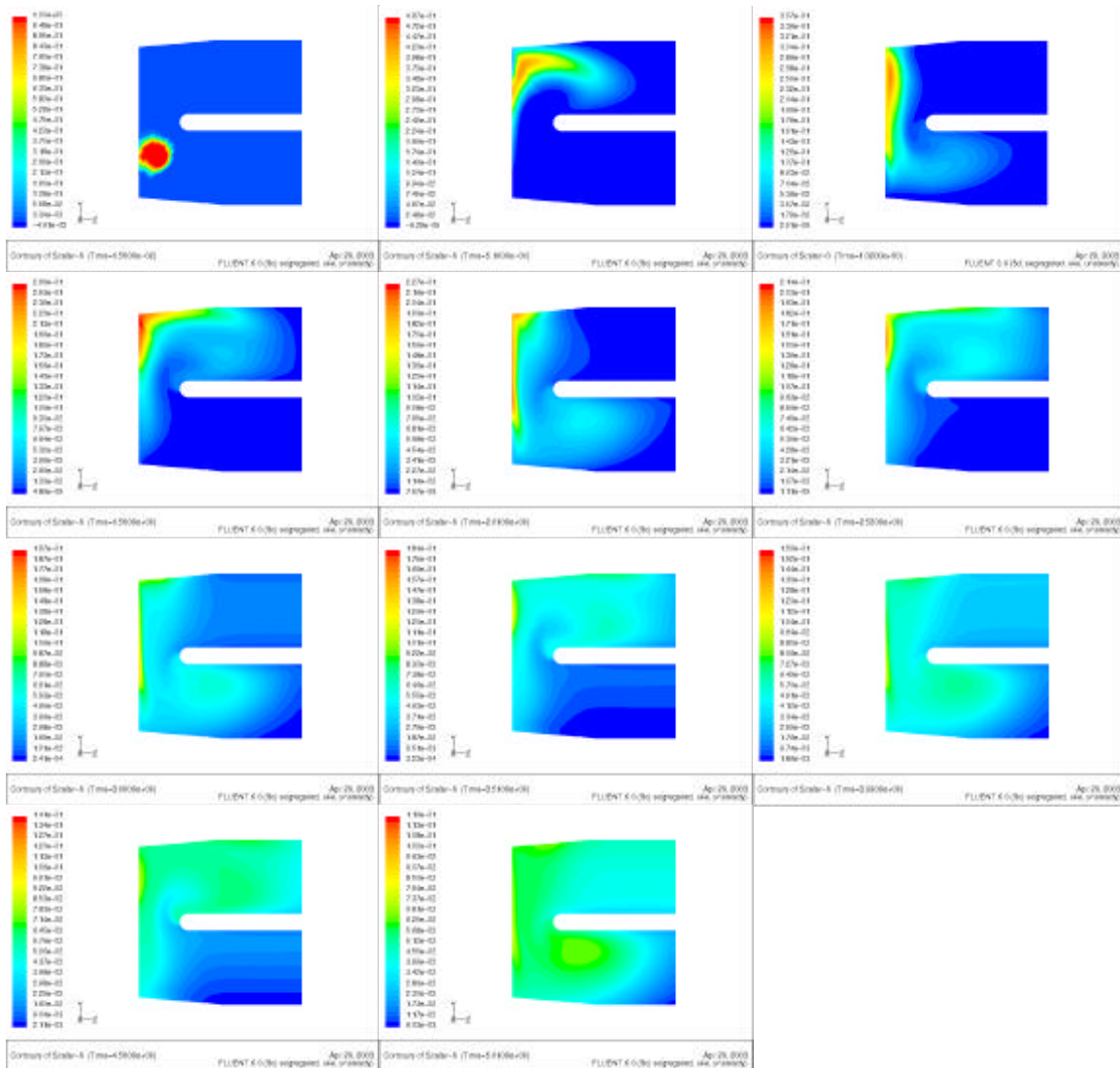


Figure 11. Relative oxygen concentration contours on center plane.

$H = 1.27$ cm, $f = 1.0$ Hz, $V = 1.5$ cc.

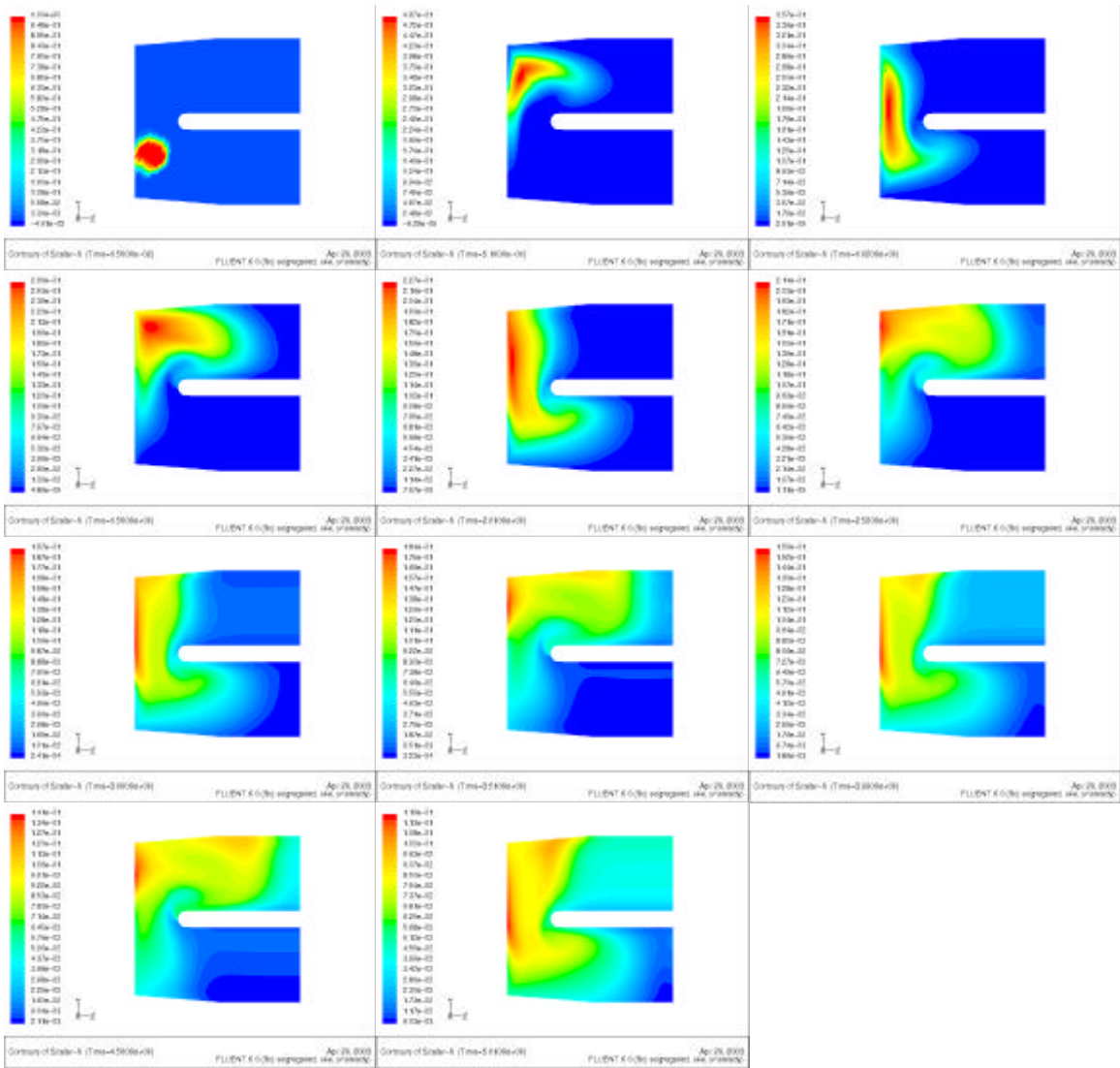


Figure 12. Relative oxygen concentration contours on bag wall.

$H = 1.27 \text{ cm}$, $f = 1.0 \text{ Hz}$, $V = 1.5 \text{ cc}$.

Figure 13 shows another way of viewing the frequency dependence. The concentration contours after three complete cycles is shown for oscillation frequencies of 0.1, 0.3, and 1.0 Hz. The corresponding contours at the center plane and bag wall are quite similar. The concentration ranges are slightly different, with the low frequencies being better mixed (14% variation versus 19%). This can be understood as more time for diffusion (30 s versus 3 s) for the 0.1-Hz compared with the 1.0-Hz case. This shows that it is primarily the number of cycles of oscillation that is important for mixing, rather than the frequency of oscillation.

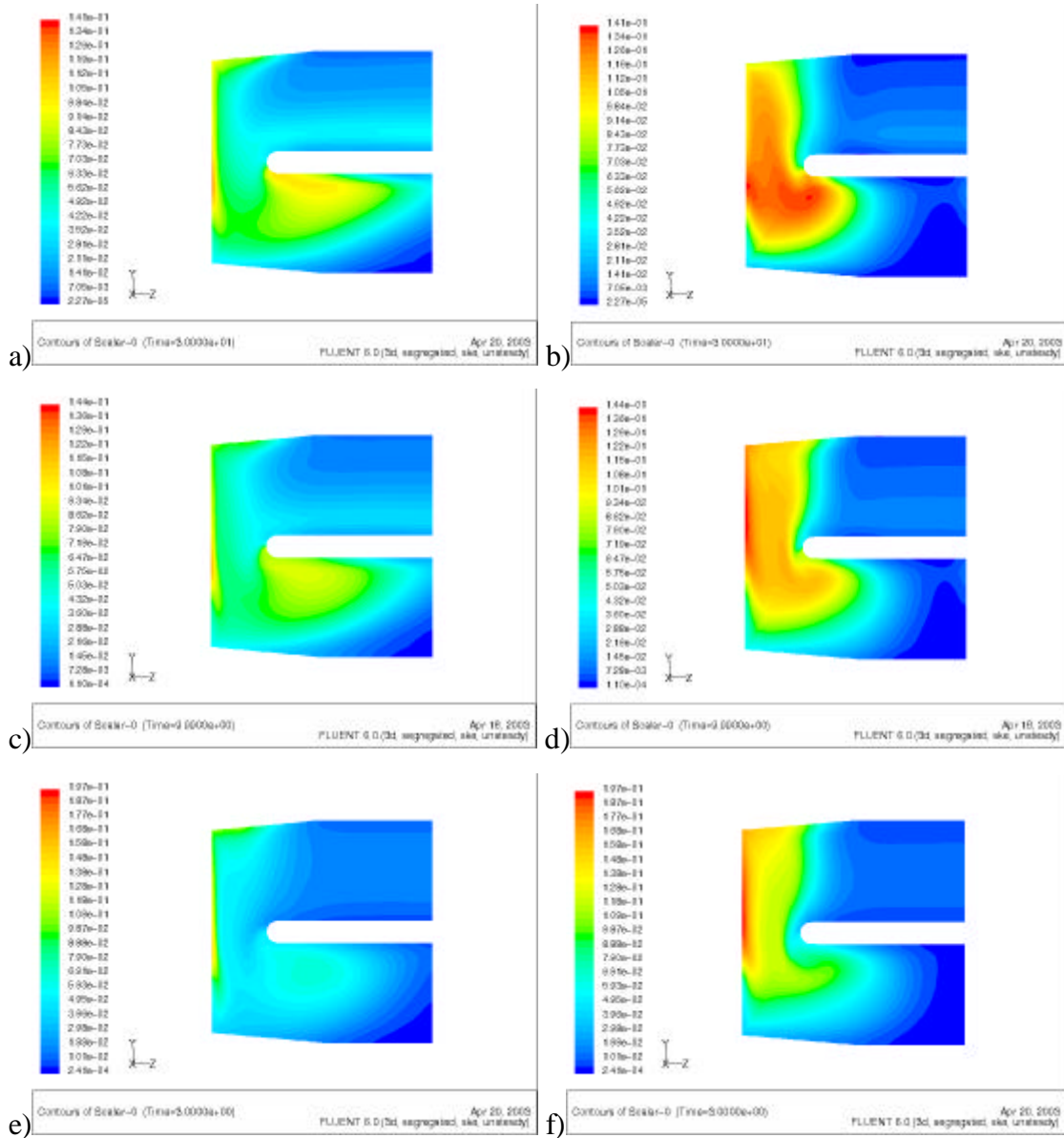


Figure 13. Relative oxygen concentration contours $H = 1.27$ cm, $V = 1.5$ cc,
a) center plane $f = 0.1$ Hz, b) bag wall $f = 0.1$ Hz, c) center plane $f = 0.3$ Hz,
d) bag wall $f = 0.3$ Hz, e) center plane $f = 1.0$ Hz, f) bag wall $f = 1.0$ Hz.

Effects of Amplitude of Oscillation on Mixing

Shown in Figure 14 are the concentration contours at 9.99 s for $H = 0.76$ cm, $f = 0.3$ Hz, and $V = 1.0, 1.5,$ and 2.0 cc. As expected, the large amplitude cases provide better distribution of the oxygen, as well as better mixing as indicated by the reduced concentration ranges as V is increased. However, it must be remembered that the

horizontal concentration contours extending from the inlets into the legs are an artifact of the imposed boundary condition and should be ignored. Still, the improvements in mixing are evident. It should also be recognized that increased amplitude also will cause higher shear levels, as shown below.

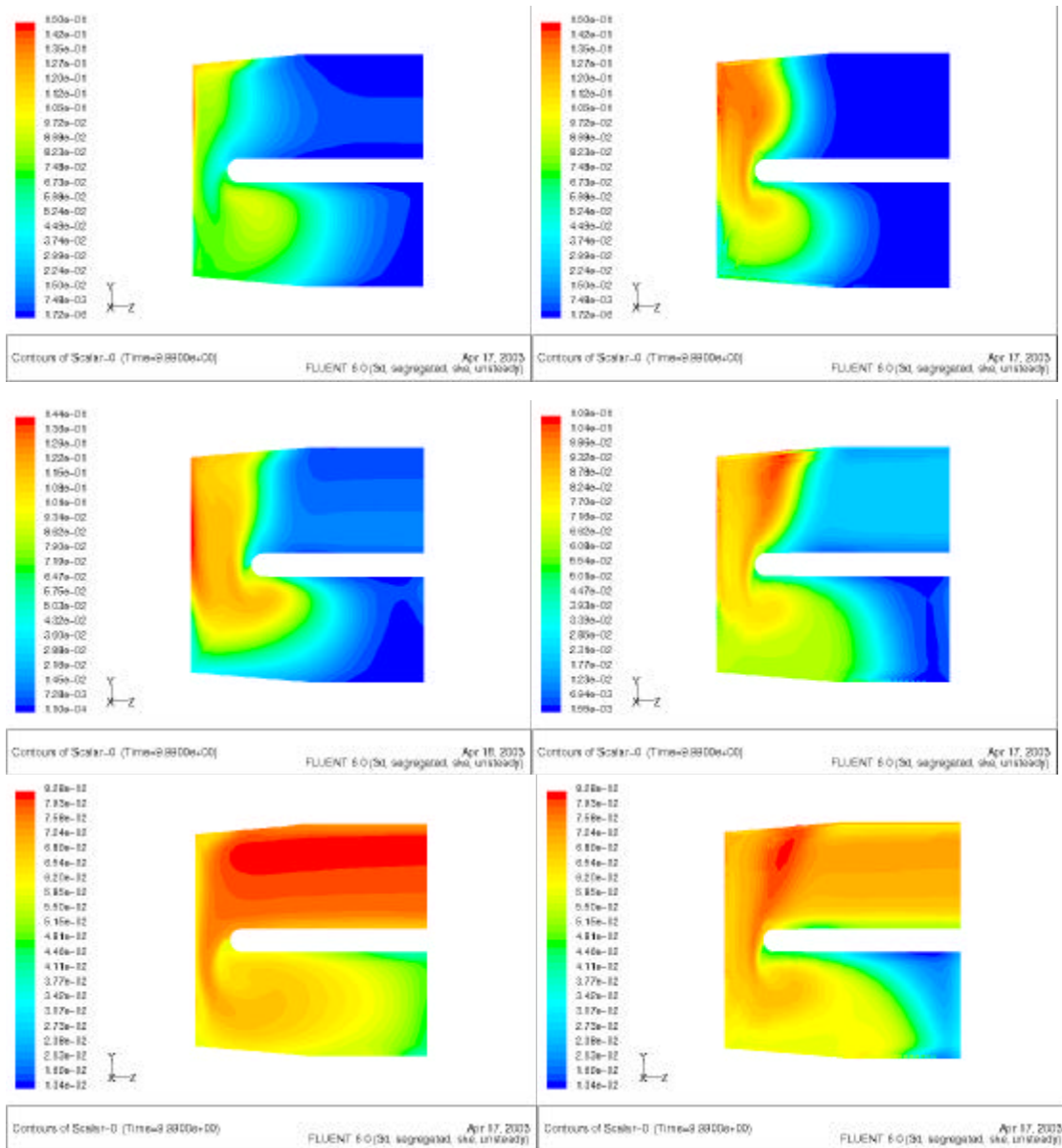


Figure 14. Relative oxygen concentration contours $H = 0.76$ cm, $f = 0.3$ Hz, a) center plane $V = 1.0$ cc, b) bag wall $V = 1.0$ cc, c) center plane $V = 1.5$ cc, d) bag wall $V = 1.5$ cc, e) center plane $V = 2.0$ cc, f) bag wall $V = 2.0$ cc.

Shear Levels

Thus far, it has been shown that the mixing process roughly scales by the strain rate and amplitude of oscillation. A simple analysis of the stress levels in the fluid media suggests that the stress increases linearly with the velocity scale. For the region between the partition tip and the header block, the velocity should scale linearly with the oscillation amplitude (displacement volume) times oscillation frequency and inversely with the flow cross-sectional area. The flow cross-sectional area is approximately H times the gap height (L = 0.76 cm). The flow velocity parameter can be defined as

$$U = \frac{Vf}{HL}$$

The velocity parameter for all of the cases investigated and the maximum wall shear stress levels obtained from the wall shear stress contours are shown in Table 1. The most striking observation from these results is that the maximum shear levels are very low, being < 0.1 dyne/cm² for all cases. This is well below the levels generally accepted as doing damage to mammalian cells [5, 6, 7, 8]. In addition, these levels occur only for short periods and only in a small region of the domain, near the partition tip. The majority of the domain is much below even this low level.

Table 1. Maximum Wall Shear Stress Levels and Computed Velocity Parameters

H (cm)	F (Hz)	V (cc)	Max. shear (dyne/cm ²)	Vel. parameter (cm/s)
1.27	1.0	2.0	0.0614	2.207
0.76	0.3	1.5	0.020	0.828
1.27	0.3	1.5	0.0107	0.497
1.27	1.0	1.5	0.044	1.655
1.27	0.1	1.5	0.0024	0.166
0.76	1.0	2.0	0.080	3.678
0.76	0.3	1.0	0.012	0.552
0.76	0.3	2.0	0.029	1.103
1.02	1.0	3.0	0.100	4.138

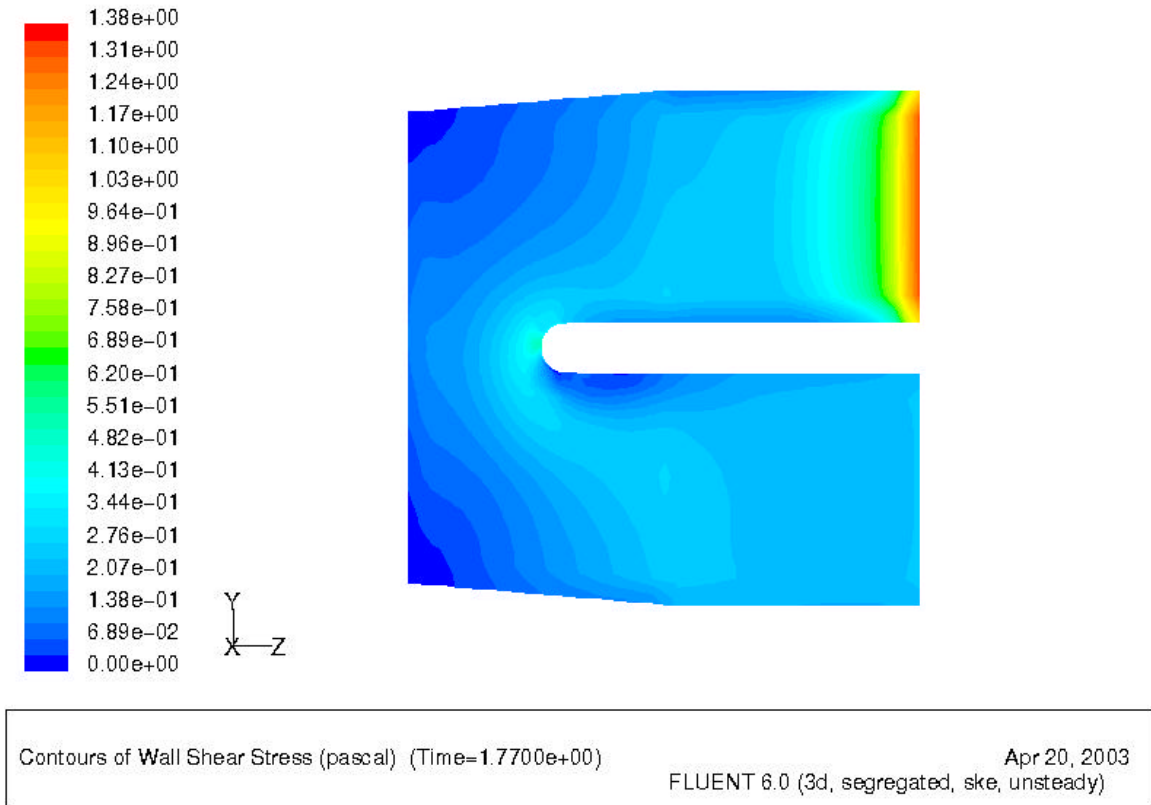


Figure 15. Wall shear stress contours at maximum shear. $H = 1.27 \text{ cm}$, $f = 1.0 \text{ Hz}$,
 $V = 1.5 \text{ cc}$.

Figure 15 shows a typical wall shear stress contour plot used to estimate the peak shear levels. The high stress levels at the upper inlet must be ignored because it is simply an artifact of the imposed uniform velocity condition at the flow exit (during this part of the oscillation cycle). The physically unrealistic uniform flow condition leads to high apparent stresses. The maximum stress level actually occurs on the partition surface near the tip. The value is estimated as 0.44 Pascal or 0.044 dyne/cm^2 from the color bar on the left.

Figure 16 shows the maximum wall shear stress level from Table 1 for all of the cases investigated plotted versus the velocity parameter. This figure shows excellent collapse of the cases to a single straight line when plotted versus the velocity parameter.

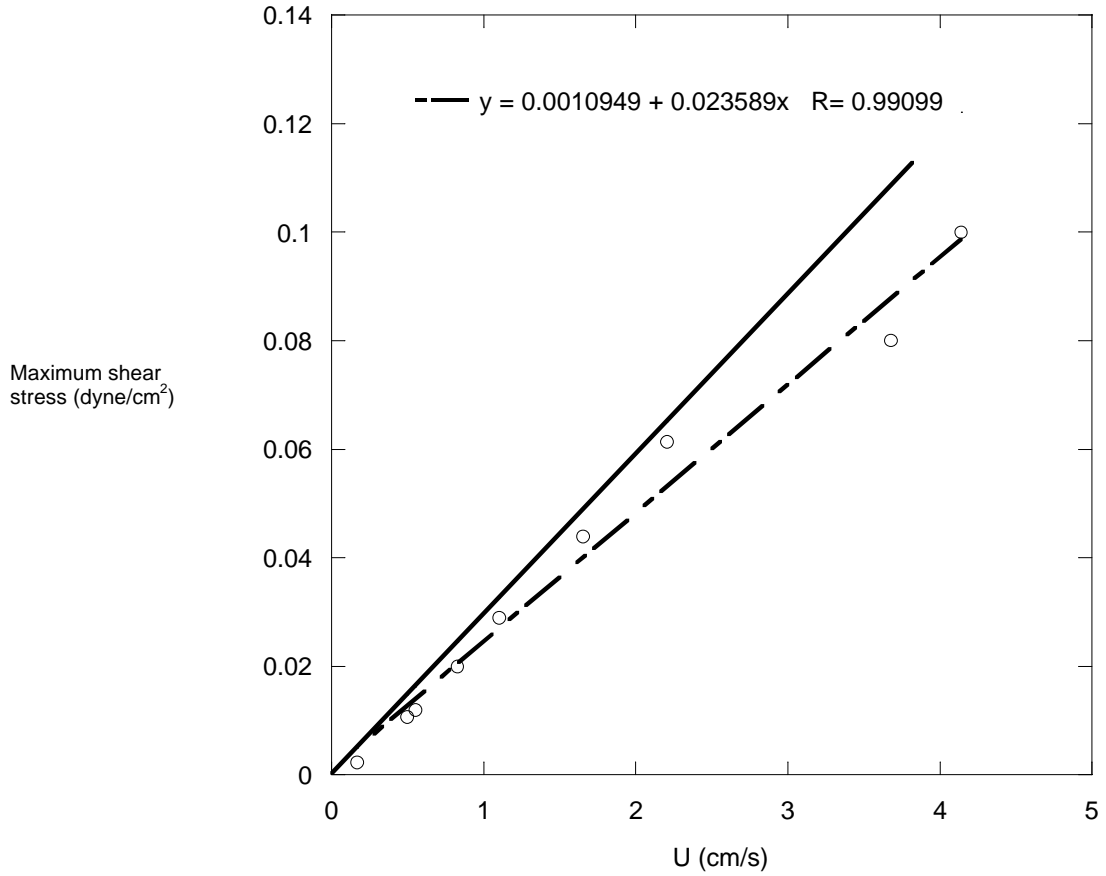


Figure 16. Maximum wall shear stress versus flow velocity parameter.

The relatively large scatter in the figure is due to the large uncertainty of identifying the stress level associated with a particular color on the color bar. The linear curve fit is shown by the dashed line and equation, while the solid line corresponds to the wall shear stress computed from an assumed parabolic velocity profile with the same flow rate across the partition gap. These results indicate that the shear stresses are near those predicted by a quasi-steady, two-dimensional model.

Conclusions

From our findings, we derive the following conclusions:

- Some form of active mixing is very important for distribution of infused scalars in the ASCS culture bags. Without mixing, scalars will take several hours to diffuse to a reasonably uniform distribution. This would most likely have serious consequences both to the viability and quality of cell cultures. Mixing will be

useful in several aspects of the culture: inoculation, feeding, and fixing of the culture. In addition, periodic mixing might be desirable during cultures.

- The partition location has only a minor affect on the mixing efficiency.
- The mixing efficiency is affected most by the number of oscillations and oscillation amplitude. This results in the mixing time being inversely related to the oscillation frequency.
- The proposed mixing protocol is very effective over the range of parameters tested. The mixing times using the protocol is approximately the time to complete 10 cycles of the oscillatory motion. This time is measured in seconds, compared with many hours required without mixing.
- The amplitude of oscillation will most likely be limited by the volume of fluid available in the deformable legs in an actual design. The results indicate this should not be a problem, since effective mixing can be accomplished at lower amplitudes with increased oscillations.

Note: *It is extremely important that the fluid in the legs be protected from stresses associated with squeezing by limiting the travel of the motion.*

- The proposed protocol produces very low mechanical shear stress levels. The results shown in Figure 16 can be used to estimate the maximum shear stress level to be expected in the bag. Since all of the parameter values tested produce very effective mixing, the frequency and amplitude of oscillation will most likely be dictated by the design of the mechanical mixing mechanism. Figure 16 then can be used to find the expected shear levels.

References

1. Schlichting, H., *Boundary Layer Theory*, seventh ed., McGraw-Hill, 1979.
2. Mills, A. F., *Basic Heat and Mass Transfer*, Irwin, 1995.
3. FLUENT 6 Tutorial Guide, Fluent Inc., Dec. 2001.
4. FLUENT 6 UDF User's Guide, Fluent Inc., Dec. 2001

5. Goodwin, T.J., Jessup J.M., Wolf, D.A., and Spaulding GF. "Reduced Shear Stress: a major component in the ability of mammalian tissues to form three-dimensional assemblies in simulated microgravity," *J Cell Biochem* 51:304-311, 1993.
6. Stathopoulos, N.A. and Hellums, J.D., "Shear stress effects on human embryonic kidney cells in vitro," *Biotechnology and Bioengineering*, Vol. 27, 1021-1026, 1985.
7. Sato, M., Levesque, M.J., and Nerem, R.M., Proceedings of Biomechanics Symposium, pp. 167-169, ASME summer meeting, 1985.
8. de Souza, P.A., Levesque, M.J., and Nerem, R.M., ASME Fluids Engineering Division Proc. 45, 471, 1986.

REPORT DOCUMENTATION PAGE			Form Approved OMB No. 0704-0188	
Public reporting burden for this collection of information is estimated to average 1 hour per response, including the time for reviewing instructions, searching existing data sources, gathering and maintaining the data needed, and completing and reviewing the collection of information. Send comments regarding this burden estimate or any other aspect of this collection of information, including suggestions for reducing this burden, to Washington Headquarters Services, Directorate for Information Operations and Reports, 1215 Jefferson Davis Highway, Suite 1204, Arlington, VA 22202-4302, and to the Office of Management and Budget, Paperwork Reduction Project (0704-0188), Washington, DC 20503.				
1. AGENCY USE ONLY (Leave Blank)	2. REPORT DATE January 2004	3. REPORT TYPE AND DATES COVERED NASA Technical Memorandum		
4. TITLE AND SUBTITLE Automated Static Culture System Cell Module Mixing Protocol and Computational Fluid Dynamics Analysis			5. FUNDING NUMBERS	
6. AUTHOR(S) Stanley J. Kleis, Ph.D.*, Tuan Truong, Thomas J. Goodwin, Ph.D.				
7. PERFORMING ORGANIZATION NAME(S) AND ADDRESS(ES) Lyndon B. Johnson Space Center Houston, Texas 77058			8. PERFORMING ORGANIZATION REPORT NUMBERS S-921	
9. SPONSORING/MONITORING AGENCY NAME(S) AND ADDRESS(ES) National Aeronautics and Space Administration Washington, DC 20546-0001			10. SPONSORING/MONITORING AGENCY REPORT NUMBER TM-2004-212067	
11. SUPPLEMENTARY NOTES *University of Houston, Houston, Texas				
12a. DISTRIBUTION/AVAILABILITY STATEMENT Unclassified/Unlimited Available from the NASA Center for AeroSpace Information (CASI) 7121 Standard Hanover, MD 21076-1320 Subject code: 23			12b. DISTRIBUTION CODE	
13. ABSTRACT (Maximum 200 words) This report is a documentation of a fluid dynamic analysis of the proposed Automated Static Culture System cell module mixing protocol. The report consists of a review of some basic fluid dynamics principles appropriate for the mixing of a patch of high oxygen content media into the surrounding media which is initially depleted of oxygen, followed by a computational fluid dynamics study of this process for the proposed protocol over a range of the governing parameters. The time histories of oxygen concentration distributions and mechanical shear levels generated are used to characterize the mixing process for different parameter values.				
14. SUBJECT TERMS fluid dynamics analysis; static culture system; computational fluid dynamics; fluid mechanics			15. NUMBER OF PAGES 32	16. PRICE CODE
17. SECURITY CLASSIFICATION OF REPORT Unclassified	18. SECURITY CLASSIFICATION OF THIS PAGE Unclassified	19. SECURITY CLASSIFICATION OF ABSTRACT Unclassified	20. LIMITATION OF ABSTRACT Unlimited	
